Free-standing terahertz chiral meta-foils exhibiting strong optical activity and negative refractive index

Jianfeng Wu,[1,a)] Binghao Ng,[2] Shuvan P. Turaga,[1] Mark B. H. Breese,[1,3] Stefan A. Maier,[2] Minghui Hong,[4] Andrew A. Bettiol,[1] and Herbert O. Moser[5]
[1]*Department of Physics, Center for Ion Beam Applications (CIBA), National University of Singapore, 2 Science Drive 3, 117542 Singapore*
[2]*Department of Physics, Imperial College, London SW7 2AZ, United Kingdom*
[3]*Singapore Synchrotron Light Source (SSLS), National University of Singapore, 5 Research Link, 117603 Singapore*
[4]*Department of Electrical and Computer Engineering, National University of Singapore, 4 Engineering Drive 3, 117576 Singapore*
[5]*Karlsruhe Institute of Technology (KIT), Network of Excellent Retired Scientists (NES), and Institute of Microstructure Technology (IMT), Postfach 3640, 76021 Karlsruhe, Germany*

(Received 6 August 2013; accepted 15 September 2013; published online 30 September 2013)

A chiral meta-foil consisting of a self-supported square array of interconnected conjugated rosettes is demonstrated at terahertz frequencies. It exhibits strong optical activity and circular dichroism. Negative refractive index with a figure-of-merit as high as 4.2 is achieved, attributed to its free-standing nature. Experimental results are in good agreement with numerical simulation. Free-standing chiral meta-foils provide a unique approach to create a completely all-metal chiral metamaterial, which can be flexibly integrated into optical setups while eliminating dielectric insertion losses. © *2013 AIP Publishing LLC*. [http://dx.doi.org/10.1063/1.4823594]

Chiral metamaterials (CMMs) were proposed as an alternative route to achieve negative refraction by Tretyakov *et al.*[1] and Pendry,[2] since a strong chiral response can push the effective refractive index of metamaterials below zero. Meanwhile, CMMs possess a rich variety of electromagnetic (EM) properties, such as optical activity, circular dichroism, and negative refraction, making them as ideal candidates for elements in optical setups.[1–20] Due to the lack of any mirror symmetry of CMMs, the magnetic and electric moments can be excited by the external electric and magnetic field components of incident EM waves, which is the basis of these special EM properties. In order to realize these EM properties, many chiral structures, such as twisted rosettes,[3–5] U-shaped split-ring resonators,[6–8] twisted cross-wires,[9,10] complementary designs,[11,12] and a conjugated gammadion,[13] have been reported. Most of these CMMs were fabricated in the GHz or near infrared frequency regimes using dielectric materials for various support functions, such as spacers between metal layers, matrices for embedding metallic resonator structures, or as substrates. Recently, metamaterial structures fabricated on ultrathin silicon nitride substrates have been demonstrated to possess significantly better performance than those fabricated on bulk silicon substrates.[21] Furthermore, THz left-handed meta-foils were first proposed to be all-metal left-handed metamaterials which can be used over a wide spectral range without unwanted substrate or matrix influences.[22] Hence, the performance of CMMs can be further improved by eliminating losses due to dielectric inclusions. Terahertz (1–10 THz) is a unique frequency range with many important applications such as security detection and gas phase molecule sensing.[23] However, it is the least explored frequency regime in the EM spectrum due to the lack of strong sources and sensitive detectors.[24] Metamaterials help to fill the technological gap, allowing the development of optical elements with unusual optical properties. Recently, some CMM designs have been investigated to achieve the unusual optical functionalities at terahertz frequencies.[16–20]

In this paper, we first propose an all-metal, self-supported, free-standing chiral metamaterial, called a chiral meta-foil (CMF), at THz frequencies. We investigate both experimentally and numerically THz CMF properties, such as strong optical activity, circular dichroism, and negative refractive index with a high figure-of-merit. Flexible CMF opens up the possibility of extending metamaterials to real three-dimensional form or bulk metamaterials, allowing more potential designs and applications than metamaterials on rigid substrates.

A CMF was constructed by a square array of conjugated rosettes interconnected with metallic wires and pillars between rosettes as shown in Fig. 1. Metallic pillars were placed between the conjugated rosettes on the top and bottom layers to make the whole structure self-supported and free-standing, whose position was shown by the black dotted lines in Fig. 1(b). The CMF could be viewed as a composite chiral metamaterial. Conjugated rosettes were arranged to break the mirror symmetry along the direction perpendicular to the metamaterial plane. The lack of mirror symmetry is an inherent property of our design, allowing that the cross-coupling between the electric and magnetic fields creates a strong chiral response around the resonance frequencies. Furthermore, we selected a conjugated structure because it has a relatively large chirality and at the same time a relatively weak electric resonance.[14]

Three-level photolithography with precise alignment and three repeated gold electroplating steps with accurate thickness control were employed to fabricate the CMF. Three optical masks, each carrying the design patterns of

[a)]Author to whom correspondence should be addressed. Electronic mail: a0051205@nus.edu.sg.

the individual layers and alignment marks, were used in the photolithography process. A 500 μm thick silicon wafer was first cleaned and covered with thin layers of Cr/Au (100 nm/50 nm) as an adhesion and plating base, respectively. A 5 μm thick AZ9260 resist was deposited by spin coating and then exposed by UV light. After resist development, the remaining resist mold was used for gold electroplating to build up a 5 μm thick gold structure. Another 50 nm Au layer was sputtered on the sample as a new plating base for the fabrication of the second and third layers of the three-dimensional structure. Next, the AZ9260 resist and Au plating bases were removed step by step using acetone and gold etchant. Finally, the whole structure was released from the silicon substrate by Cr etching to form all-metal free-standing chiral metamaterials. Figures 1(a) and 1(b) show 3D schematics of CMF and its geometry parameters. Figure 1(c) shows a photograph of the CMF, in which the useful window is 10 mm × 10 mm × 0.015 mm (L × W × H). Figures 1(d) and 1(e) show scanning electron microscope (SEM) images of the fabricated CMF.

The fabricated CMF was characterized by terahertz-time-domain spectroscopy (THz-TDS) in a nitrogen purged chamber with a relative humidity less than 5%. Time-domain spectra of the co- and cross-polarization states of the CMF were measured in transmission mode by employing polyethylene polarizers (TYDEX) before and after the CMF. Transmission coefficients of the circularly polarized waves were then obtained from the linear polarization measurements using the following equation:

$$\begin{pmatrix} T_{++} & T_{+-} \\ T_{-+} & T_{--} \end{pmatrix} = \frac{1}{2}\begin{pmatrix} (T_{xx}+T_{yy})+i(T_{xy}-T_{yx}) & (T_{xx}-T_{yy})-i(T_{xy}+T_{yx}) \\ (T_{xx}-T_{yy})+i(T_{xy}+T_{yx}) & (T_{xx}+T_{yy})-i(T_{xy}-T_{yx}) \end{pmatrix}, \quad (1)$$

where the first and second subscripts refer to the incident and transmitted waves, + and − refer to the right-handed (RCP) and left-handed circularly polarized (LCP) waves, and x and y refer to the two linearly polarized waves with the electric field polarized along two orthogonal directions.[25]

Simulations of the CMF properties were performed using the frequency domain solver of CST Microwave Studio, which implements a finite element method to determine reflection and transmission properties. In the simulation, the unit cell boundary condition was applied and the circularly polarized eigenwaves were directly used. Gold in the CMF was described as a lossy metal with conductivity $\sigma = 4.09 \times 10^7$ Sm^{-1}.

Figures 2(a) and 2(b) show the simulated and measured transmission coefficients as functions of frequency. In simulation, the transmission of the LCP wave is higher than the RCP wave around a frequency of 1.21 THz, while the transmission of the LCP wave is much lower than the RCP wave around

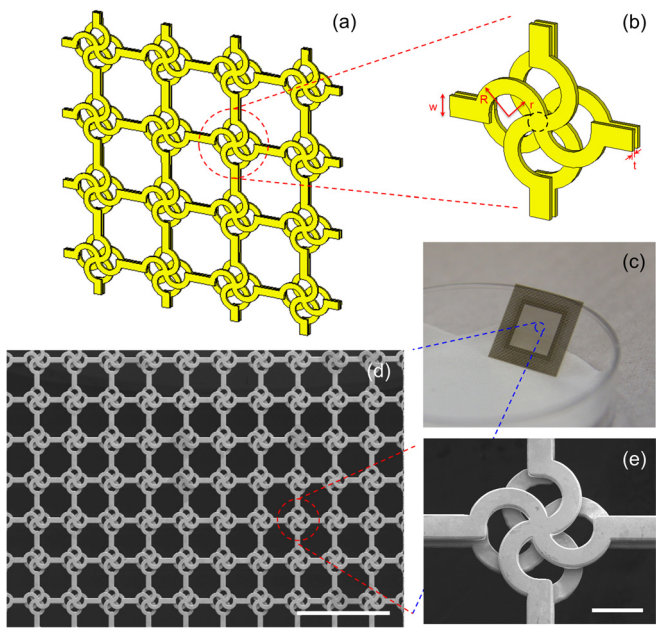

FIG. 1. (a) and (b) 3D schematics of the conjugated rosette CMF, and the geometry parameters are given by R = 40 μm, r = 24 μm, w = 22 μm, t = 5 μm, and the unit cell size u = 200 μm. The black dotted lines mark the position of pillar. (c) Photograph of the CMF. (d) and (e) SEM images of the fabricated CMF. The scale bar is 500 μm in (d) and 50 μm in (e).

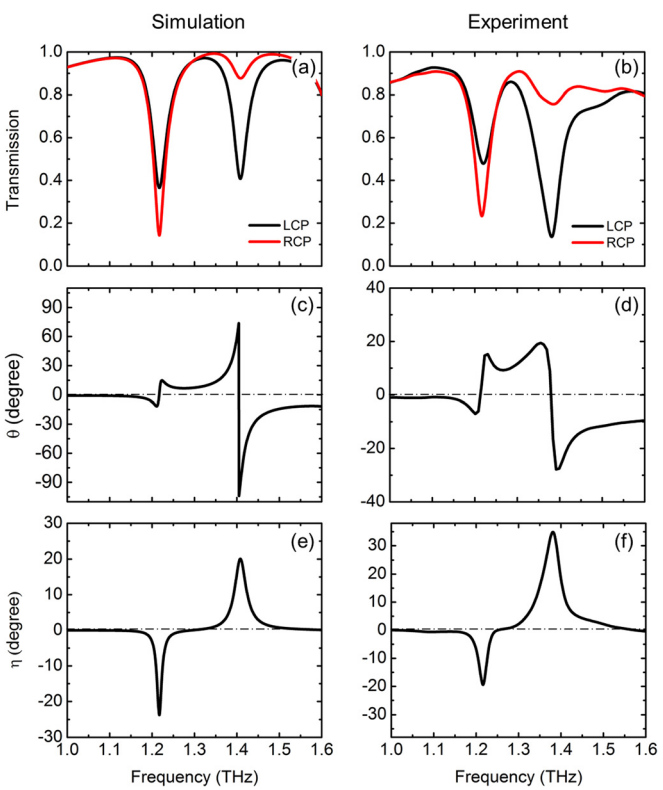

FIG. 2. Simulation (left) and experimental (right) results of the CMF. (a) and (b) The transmissions of the LCP and RCP waves. (c) and (d) The polarization azimuth rotation angle θ. (e) and (f) The ellipticity η of the transmitted wave.

1.41 THz. As shown in Fig. 2(b), the experimentally observed resonances at 1.21 THz and 1.38 THz are in good agreement with simulations. The circular dichroism, i.e., the difference between RCP and LCP transmission, reaches about 62% at 1.38 THz in the measured results. Note that small discrepancies exist between experiment and simulation, we conjecture that they are mainly due to the tolerance in the fabrication and characterization. Using the standard definition of the polarization azimuth rotation $\theta = [\arg(T_{++}) - \arg(T_{--})]/2$, and the ellipticity $\eta = \arctan[(|T_{++}| - |T_{--}|)/(|T_{++}| + |T_{--}|)]$,[11,26] we calculate the polarization changes in a linearly polarized wave incident on the chiral meta-foils shown in Figs. 2(c)–2(f). At the resonant frequencies of 1.21 THz and 1.41 THz, the azimuth rotation and ellipticity reach their maximum values, ($\theta = -12°$, $\eta = -24°$) and ($\theta = -104°$, $\eta = 20°$), respectively. Meanwhile, it is clearly observed that, in the middle of the two resonant frequencies, the ellipticity $\eta = 0$, which corresponds to the pure optical activity effect. That is, for a linearly polarized incident wave, the transmitted wave is still linearly polarized with a polarization rotated by an angle θ. For the CMF, we observe a polarization rotation of 10° with $\eta = 0$. The origin of the chiral response of the conjugated structures has been discussed by a procedure of transmutation from the simple Ω-particle chiral element to the conjugated chiral metamaterials.[13,14] Magnetic or electric moments are induced by the electric or magnetic fields, respectively, of the incident electromagnetic wave in the antiparallel or parallel direction. The conjugated arrangement breaks the mirror symmetry in the direction perpendicular to the plane of the metamaterial, and thereby induces strong chirality around the resonance frequencies.

Using the simulated transmission and reflection data, we calculate the effective constitutive parameters of the CMF.[15] The effective impedance z and refractive index $n_{\pm}$ are given as

$$z = \pm\sqrt{\frac{(1+R)^2 - T_+T_-}{(1-R)^2 - T_+T_-}}, \tag{2}$$

$$n_{\pm} = \frac{i}{k_0 d}\left\{\ln\left[\frac{1}{T_{\pm}}\left(1 - \frac{z-1}{z+1}R\right)\right] \pm 2m\pi\right\}. \tag{3}$$

The sign of the square root in Eq. (2) and the multi-branches in Eq. (3) need to be chosen carefully according to the energy conservation principle, i.e., $\mathrm{Re}(z) \geq 0$, $\mathrm{Im}(n) \geq 0$. Once z and $n_{\pm}$ are calculated, the other parameters can be identified subsequently, $\kappa = (n_+ - n_-)/2$, $n = (n_+ + n_-)/2$, $\mu = nz$, $\varepsilon = \frac{n}{z}$, where κ is the chirality parameter, n is the refractive index, ε and μ are the permittivity and permeability, respectively. The strong chirality can easily push the refractive index of the RCP/LCP eigenwaves, $n_{\pm} = n \pm \kappa$, to be negative at the two resonances, especially at the higher resonance, seen in the shaded regions of Fig. 3 from 1.23 to 1.31 THz for n_+ and from 1.42 to 1.49 THz for n_-. The amplitude of the chirality κ at off-resonance frequencies around 1.3 THz is about 0.3, which is enormous compared to natural materials such as sugar and quartz, where κ is around 10^{-5}. The efficiency of the negative refractive index is usually characterized by the figure of merit (FOM), which is defined as FOM = -Re(n)/Im(n). For RCP light, the negative refractive index region around 1.21 THz has a maximum FOM = 2.8, while for LCP light, the negative refractive index region around 1.41 THz has a maximum FOM = 4.2. These values are much higher than those reported earlier.[3–13] Most chiral structures were fabricated on substrates such as flame-resistant grade 4 board or other photopolymers which have an associated large loss to decrease the FOM value. However, the CMF is an all-metal self-supported free-standing chiral metamaterial structure which properties are solely determined by the geometric structure and the metal properties. Since it is free from limitations imposed by the substrates, the CMF can be optimized to achieve a much higher FOM value to become a more suitable chiral design with a negative index.

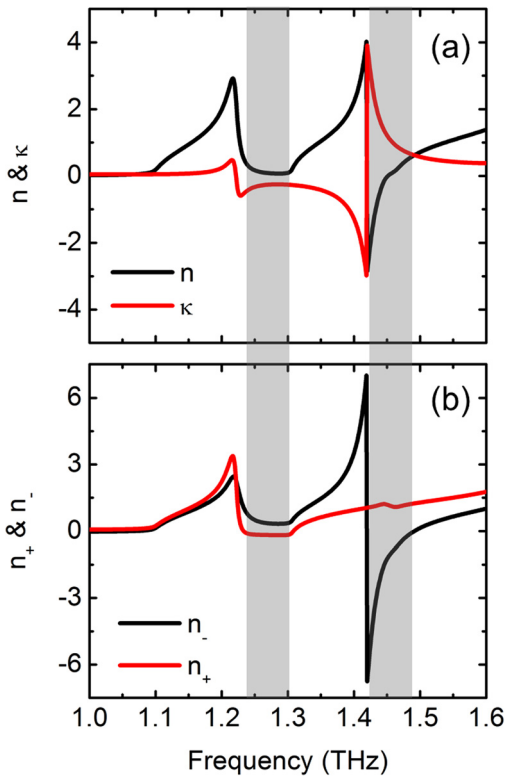

FIG. 3. Retrieved effective parameters of the CMF based on the simulation data. (a) Real parts of the refractive index n and chirality κ. (b) Real parts of the refractive indices for the LCP and RCP waves.

In conclusion, we experimentally and numerically demonstrate a conjugated rosette, chiral meta-foil that exhibits strong optical activity, circular dichroism, and negative refractive index with a high figure-of-merit. Free-standing chiral meta-foils provide a unique approach to create a completely all-metal chiral metamaterial, which can be flexibly integrated with other terahertz functional materials and devices. Furthermore, all-metal bulk CMMs are possible to be realized by via layer-by-layer method.

This work was supported by the NUS Core Support C-380-003-003-001, and the funding provided by the EPSRC and the Leverhulme Trust.

[1]S. Tretyakov, I. Nefedov, A. Sihvola, S. Maslovski, and C. Simovski, J. Electromagn. Waves Appl. **17**, 695 (2003).
[2]J. B. Pendry, Science **306**, 1353 (2004).

[3]A. V. Rogacheva, V. A. Fedotov, A. S. Schwanecke, and N. I. Zheludev, Phys. Rev. Lett. **97**, 177401 (2006).
[4]E. Plum, V. A. Fedotov, A. S. Schwanecke, N. I. Zheludev, and Y. Chen, Appl. Phys. Lett. **90**, 223113 (2007).
[5]E. Plum, J. Zhou, J. Dong, V. A. Fedotov, T. Koschny, C. M. Soukoulis, and N. I. Zheludev, Phys. Rev. B **79**, 035407 (2009).
[6]Z. Li, R. Zhao, T. Koschny, M. Kafesaki, K. B. Alici, E. Colak, H. Caglayan, E. Ozbay, and C. M. Soukoulis, Appl. Phys. Lett. **97**, 081901 (2010).
[7]X. Xiong, W. H. Sun, Y. J. Bao, M. Wang, R. W. Peng, C. Sun, X. Lu, J. Shao, Z. F. Li, and N. B. Ming, Phys. Rev. B **81**, 075119 (2010).
[8]M. Decker, R. Zhao, C. M. Soukoulis, S. Linden, and M. Wegener, Opt. Lett. **35**, 1593 (2010).
[9]J. Zhou, J. Dong, B. Wang, T. Koschny, M. Kafesaki, and C. M. Soukoulis, Phys. Rev. B **79**, 121104 (2009).
[10]M. Decker, M. Ruther, C. E. Kriegler, J. Zhou, C. M. Soukoulis, S. Linden, and M. Wegener, Opt. Lett. **34**, 2501 (2009).
[11]Z. Li, K. B. Alici, E. Colak, and E. Ozbay, Appl. Phys. Lett. **98**, 161907 (2011).
[12]K. Hannam, D. A. Powell, I. V. Shadrivov, and Y. S. Kivshar, Appl. Phys. Lett. **102**, 201121 (2013).
[13]R. Zhao, L. Zhang, J. Zhou, T. Koschny, and C. M. Soukoulis, Phys. Rev. B **83**, 035105 (2011).
[14]R. Zhao, T. Koschny, E. N. Economou, and C. M. Soukoulis, Phys. Rev. B **81**, 235126 (2010).
[15]R. Zhao, T. Koschny, and C. M. Soukoulis, Opt. Express **18**, 14553 (2010).
[16]R. Singh, E. Plum, C. Menzel, C. Rockstuhl, A. K. Azad, R. A. Cheville, F. Lederer, W. Zhang, and N. I. Zheludev, Phys. Rev. B **80**, 153104 (2009).
[17]S. Zhang, Y.-S. Park, J. Li, X. Lu, W. Zhang, and X. Zhang, Phys. Rev. Lett. **102**, 023901 (2009).
[18]S. Zhang, J. Zhou, Y.-S. Park, J. Rho, R. Singh, S. Nam, A. K. Azad, H.-T. Chen, X. Yin, A. J. Taylor, and X. Zhang, Nature Commun. **3**, 942 (2012).
[19]G. Kenanakis, R. Zhao, A. Stavrinidis, G. Konstantinidis, N. Katsarakis, M. Kafesaki, C. M. Soukoulis, and E. N. Economou, Opt. Mater. Express **2**, 1702 (2012).
[20]C. M. Soukoulis and M. Wegener, Nature Photon. **5**, 523 (2011).
[21]H. Tao, A. C. Strikwerda, M. Liu, J. P. Mondia, E. Ekmekci, K. Fan, D. L. Kaplan, W. J. Padilla, X. Zhang, R. D. Averitt, and F. G. Omenetto, Appl. Phys. Lett. **97**, 261909 (2010).
[22]H. O. Moser, L. K. Jian, H. S. Chen, M. Bahou, S. M. P. Kalaiselvi, S. Virasawmy, S. M. Maniam, X. X. Cheng, S. P. Heussler, S. B. Mahmood, and B. I. Wu, Opt. Express **17**, 23914 (2009).
[23]X. C. Zhang, Phys. Med. Biol. **47**, 3667 (2002).
[24]C. A. Schmuttenmaer, Chem. Rev. **104**, 1759 (2004).
[25]J. A. Kong, *Electromagnetic Wave Theory* (EMW, Cambridge, 2008).
[26]J. D. Jackson, *Classical Electrodynamics*, 3rd ed. (Wiley, New York, 1998).